

Green Hydrogen Production: Process Design and Capacity Expansion Integrating Economic and Operational Autonomy Objectives

Andrés I. Cárdenas, Felipe A. Díaz-Alvarado,* and Ana Ines Torres



Cite This: <https://doi.org/10.1021/acs.iecr.3c03060>



Read Online

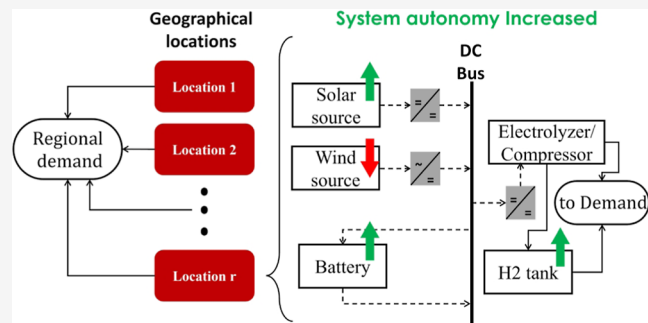
ACCESS |

Metrics & More

Article Recommendations

Supporting Information

ABSTRACT: Green hydrogen is an attractive energy vector due to its zero carbon emission in production and use, supporting many industries in their transition to cleaner operations. However, the production of green hydrogen has a fundamental challenge in resilience since it requires renewable energy (RE) systems that are subject to variability. This study develops an optimization-based decision-making framework for the design and capacity expansion of hydrogen production systems at a regional level. A novel resilience objective function that considers external RE-derived fluctuations as well as internal plant failures is proposed. An illustrative case study using data from five regions in Chile verifies that consideration of resiliency in the objective function results in a system that is able to overcome the variance without greatly increasing the equilibrium cost for hydrogen. These designs are based on dual-storage capacities with different expansion profiles.



INTRODUCTION

Fossil fuels and their greenhouse gas emissions have considerably impacted the environment, specifically on climate change.¹ Renewable energies (REs) are proposed to mitigate this problem; however, REs present new technical challenges compared with traditional fossil resources. For example, renewable sources are susceptible to exogenous effects such as weather conditions, making some of them unpredictable (e.g., tidal and wind energy). As a consequence, the supply has to deal with uncertainty.²

The concept of a hybrid RE system (HRES) has been developed to withstand this deficiency. It proposes that a system composed of coupled RE sources can complement each other's weaknesses and produce a more stable energy output. In addition, these systems consider various types of energy storage technologies to further improve the desired stability.³

Green hydrogen has been studied extensively as an energy carrier with no direct carbon emissions during the production phase.⁴ This attractive property has led to international interest in developing hydrogen production based on HRESs. However, dealing with the variability of RE sources is still a pending question in the regional- or national-scale HRES design phase.

A research gap exists regarding the use of resilience metrics in the design and optimization of long-term HRESs.⁵ This article proposes a metric that provides a quantitative approach to HRES resilience for green hydrogen production by considering the resource variability and the intrinsic failure rate of physical components in the system. This quantitative approach is

expressed as an objective function in an optimization problem model to decide the capacity expansion of an off-grid, regional-scale green hydrogen production system.

State of the Art: HRES Modeling and Applications.

Mathematical programming has been recently used in power systems and HRES design. For example, Siddaiah and Saini⁶ propose mathematical programming to achieve a specified goal (such as minimal cost or emissions) in HRES design while considering pertinent constraints associated with the system and its parts; Lara et al.⁷ proposed a deterministic multiscale formulation for electric power infrastructure planning, considering annual generation, investment, and hourly operational decisions; Alraddadi et al.⁸ modeled the expansion planning of power systems that incorporate a high solar power share, where higher generation and storage capacity are required to meet demand at night; Wang et al.⁹ coupled the optimization of a regionally integrated energy system together with 11 sustainability indices to a case study in Xinjiang, China; and Cho et al.¹⁰ implemented a generalized disjunctive programming strategy with a bilevel decomposition approach for reliable power system

Received: August 29, 2023

Revised: December 1, 2023

Accepted: December 5, 2023

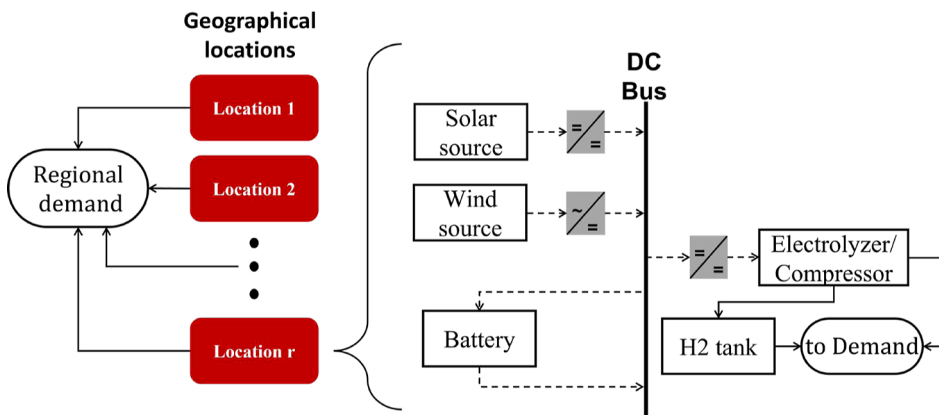


Figure 1. Graphical representation of the regional production problem. A given H₂ demand will be satisfied by r locations; each location needs to define the capacity (solar and wind generators, battery, electrolyzer, and storage tanks) to install and their expansion plan for a 15 year time horizon.

planning, determining long-term investment and short-term operational decisions.

Coupling renewable power sources with the production of renewable fuel carries over the difficulties of renewable power systems, where the intermittency of these power sources is a relevant design factor. Along these lines, Zhang et al.¹¹ integrated HRES into the planning and scheduling of renewable-based fuels and power production, identifying bottlenecks and synergies when RE sources are considered; Corengia and Torres¹² formulated a superstructure optimization model that considers the selection of energy sources, type of electrolyzer, its capacity, and energy storage devices to select the optimal green hydrogen production capacity for a given RE generation pattern. Showing that the flexibility of PEM electrolyzer does not, in general, counterbalance its higher costs; and Cooper et al.¹³ proposed a hydrogen hub designed to operate at variable operation through a bilevel optimization approach.

State of the Art: Resilience in Power Systems. Resilience can be understood as the capacity to withstand misfortune and recover from undesirable events. Applied to any specific field, such as energy systems, infrastructure, materials science, and others, this definition needs to be more specific to propose a resilience indicator. This specificity depends on the system under study. The most common approach to define resilience in an energy system is through the systems health-overtime-curve, representing the transient state of specific properties over time after an incident that disrupts a stable condition. As discussed by Gasser et al.,¹⁴ multiple resilience definitions and measures are defined through this curve. They can be clustered in two groups: draw-down, which represents the system's loss due to an undesired event, and draw-up, as the system's ability to recover from said adverse event. Some examples of the draw-down section of the curve are the following.

- Robustness: which refers to a system's capacity to withstand a given level of stress or demand without any loss of function.¹⁵
- Absorptiveness: defined as the degree to which a system can absorb the impacts of a perturbation and minimize consequences with minimal effort.¹⁶
- Resistance: which refers to the capacity of the system to stay within acceptable ranges of functionality after a negative event.¹⁷

The draw-up section of the curve is associated with recovery. Some examples are as follows.

- Recovery: refers to the capacity to recover quickly and at low cost from potentially disruptive events.^{17,18}
- Adaptability: refers to how the system adapts to the newly introduced conditions.¹⁹
- Rebuildability: refers to the capacity to rebuild all the functions and establish normal operation.²⁰

An innovative approach in considering resilience in HRES design is the one in Vera.²¹ Here, a novel resilience indicator that considers a system's capacity to recover from catastrophic events, such as earthquakes, is included as an objective function in a MILP optimization framework. Furthermore, the authors conducted a comprehensive review of resilience indicators based on the system's health over time curve and relevant indicators from other disciplines. In general, power system resilience places special attention on the dynamics of the system (noticeable through the health–overtime curve), while other disciplines such as economics, Internet networks, transportation, and water resource management have applied stationary (nontime-dependent/nondynamic) resilience metrics.^{22–25}

Another approach is included in the study of Cho et al.²⁶ where simultaneous consideration of reliability (withstanding component failure), flexibility (feasible operation under uncertain conditions), and resilience (capacity to withstand catastrophic events) in power system planning stem as a requirement for future advanced optimization.

Aim of This Study. Most of the resilience metrics described above are based on the system's health-overtime curve. Because of this, resilience metrics can be used in dynamic models for planning energy systems. Consequently, the indicators require information about how much system loss occurred at a specific time, how long it lasted, and how fast the system dropped quality and recovered functionality. When design considers long-term planning, such as capacity expansion models, it is not possible to assess with confidence which disruptive events will occur and what their magnitudes will be. This results in a research gap when optimizing HRES design with respect to robustness and resilience.⁵

This paper introduces a multidimensional design of a regional green hydrogen production system through a novel objective function for HRES operational resilience. This novel resilience metric accounts for the power source variability, internal physical component failure, and their mitigation through a dual-storage system of batteries and H₂ storage. The trade-off between an increased storage capacity, RE variability, plant allocation, and the cost of the system is analyzed through a

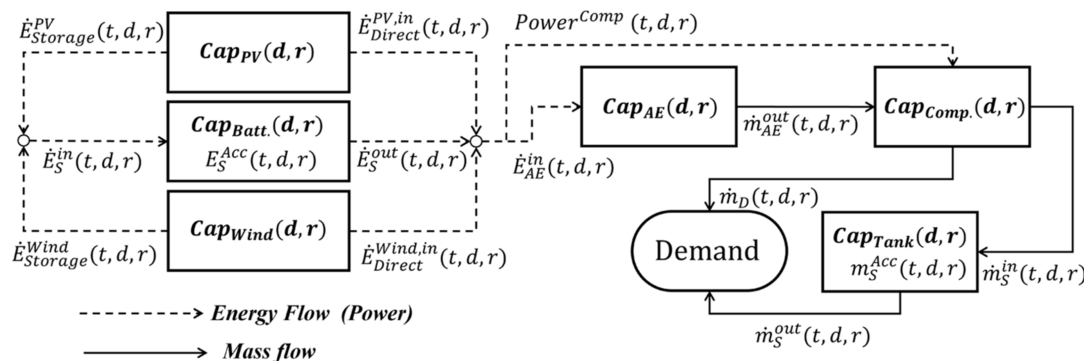


Figure 2. Superstructure for a generic solar/wind green hydrogen production plant. Solar and wind generators can supply power directly to the electrolyzer and compressor; a battery system can be placed to balance the intermittencies of the generators. The demand for hydrogen can be directly satisfied from production or intermediate storage tanks.

multiobjective optimization of the present cost and the proposed operational resilience function through a regional capacity expansion.

We consider Chile as the case study as it is known as one of the countries with a significant capacity to produce clean energy, specifically from solar and wind sources, and has the opportunity to become a global leader in green hydrogen production.²⁷

Problem Statement. This work focuses on the allocation and capacity expansion of off-grid green hydrogen production facilities within a delimited geographical region subject to a given hydrogen demand. Each location in the region needs to define whether or not to install RE (RE, solar, or wind) generators, a bank of batteries to store that energy, an electrolyzer, the associated hydrogen compression stage, and tanks for storage. In addition, we wanted these designs to be resilient. Figure 1 depicts a representation of the problem.

Due to the RE sources' intermittency, energy output variability is expected. Said variability may result in a hydrogen production deficit if the system cannot overcome the energy shortfall. Storage capacity, either in batteries or in hydrogen tanks, provides the system with flexibility in operation, reducing the effects of an energy deficit but incurring a trade-off of higher capital and operational cost. The main objective of the allocation and subsequent capacity expansion is to determine the optimal sizing and investment plan for each location each year to flourish for an economical and flexible regional hydrogen production system.

The possible processing alternatives can be represented in a superstructure, as shown in Figure 2. In there, mass and energy flows are, respectively, presented as filled and dashed lines, whereas equipment capacity variables are presented as bold text. The capacity of the equipment can vary in the time horizon. We assume that the plants do not interact with each other.

The superstructure considers that RE sources can directly supply the electrolyzer with power for hydrogen production or feed a battery system to store energy for later discharge to the electrolyzer. Alkaline electrolysis (AE) is considered in this study since it is currently the most cost-efficient technology (see the Supporting Information). Hydrogen is compressed to 30 MPa.

Formulation of an optimization problem to solve the superstructure results in a mixed integer linear programming problem that considers r locations and d days hourly discretized by the index t . A summary of the main equations of the model is given in the following subsections; a condensed model formulation is available in the Supporting Information.

MODELING

Representative Day Approach. The time horizon for design and expansion is considered to be 15 years from 2025 to 2040. Modeling hourly operations of said systems to capture detailed climatic conditions is known to turn the optimization of the system into an intractable problem.²⁸ To withstand this complication, a representative day approach is considered. This method is based on selecting specific periods of a historical year; each period is then represented by a characteristic day, which encompasses the overall behavior of the property being analyzed.²⁹ Representative day selection and time aggregation techniques that manage to accurately represent the behavior of solar and wind time series are still an open discussion;^{30,31} for this case study, 3 representative days are chosen as a means to provide reasonable computation time for the model and encompass the periods of high, intermediate, and low incidence of solar radiation and wind speed. Details are shown in the Supporting Information. Since the focus of this paper seeks to develop a methodology for operational resilience measurement as an objective function, further discussion on time aggregation techniques and the selection of representative days for the case study are not considered.

Equipment. Solar and Wind Energy Generators. RE sources are modeled according to the installed equipment area in each location on a certain representative day. The variables associated with the installed PV panel area and wind turbine swipe area are $A_{d,r}^{PV}$ and $A_{d,r}^{Wind}$, respectively. The solar energy generation model is presented in eq 1, where the output power is modeled as linearly dependent on the installed area, the solar radiation, and the panel efficiency.³²

$$\dot{E}_{PV,t,d,r}^{\text{Direct}} + \dot{E}_{PV,t,d,r}^{\text{Storage}} = \eta_{PV} \cdot A_{d,r}^{PV} \cdot G_{t,d,r}^{\text{Sun}} \quad (1)$$

The wind energy generation model in turbines follows the fact that the total output power depends on the installed swipe area, the capacity factor of the turbine, the average wind speed, and the air density,³³ as shown in eq 2.

$$\dot{E}_{Wind,t,d,r}^{\text{Direct}} + \dot{E}_{Wind,t,d,r}^{\text{Storage}} = \frac{1}{2} \cdot C_p^{\text{Wind}} \cdot A_{d,r}^{\text{Wind}} \cdot \rho_{\text{Air}} \cdot (v_{t,d,r}^{\text{Wind}})^3 \quad (2)$$

In this study, a constant height of the turbine (80 m) is assumed since an in-depth design of equipment is out of the scope of this study. Afsharian and Taylor³⁴ provide a systematic approach to relate the wind turbine swipe area with the land area

requirements; a value of $1.7 \cdot 10^{-3} \left[\frac{\text{m}^2 \text{ swipe}}{\text{m}^2 \text{ land}} \right]$ is set for the present study.

Energy Storage in Batteries. Battery systems present three relevant modeling requirements: (i) the energy balance that relates inputs, outputs, and accumulated energy, (ii) the minimal and maximal states of charge (SOCs) required to preserve the battery system's correct operation and lifetime, and (iii) logical constraint that prevents simultaneous battery charge/discharge.³⁵ The energy balance of the battery system is presented in eq 3, where the charge (η_{Charge}), discharge ($\eta_{\text{Discharge}}$), and passive losses ($[1 - L^{\text{Battery}}]$) are considered.

$$\begin{aligned} E_{t,d,r}^{\text{Acc}} = & [1 - L^{\text{Battery}}] \cdot E_{t-1,d,r}^{\text{Acc}} \\ & + \Delta t \cdot \left(\eta_{\text{Charge}} \cdot \dot{E}_{t-1,d,r}^{\text{in}} - \frac{\dot{E}_{t-1,d,r}^{\text{out}}}{\eta_{\text{Discharge}}} \right) \end{aligned} \quad (3)$$

A linear constraint for the battery systems' SOC nominal battery capacity constrains the stored energy according to the minimal and maximal SOC as presented in eq 4.

$$\text{SOC}_{\min} \cdot \text{Cap}_{\text{Battery},d,r} \leq E_{t,d,r}^{\text{Acc}} \leq \text{SOC}_{\max} \cdot \text{Cap}_{\text{Battery},d,r} \quad (4)$$

Following Corengia and Torres, 2018,³⁶ the nonsimultaneous charge/discharge is dropped as it may only be optimal in systems where negative energy prices are allowed.

Electrolyzer. We consider an alkaline electrolyzer where the mass of hydrogen produced is related to the power supply, as shown in eq 5.

$$\dot{E}_{\text{AE},t,d,r}^{\text{in}} = \frac{\dot{m}_{\text{AE},t,d,r}^{\text{out}} \cdot \Delta H}{\eta_{\text{AE}}} \quad (5)$$

Here, η_{AE} is the electrolyzer's power to hydrogen efficiency and ΔH is the water to hydrogen reaction enthalpy. The $\frac{\Delta H}{\eta_{\text{AE}}}$ factor is considered to be 57.3 kW h/kg for AE.^{37,38}

An essential characteristic of AE technologies is that at small/medium capacities, a minimum load factor is required to avoid persistent shutdown periods in the electrolyzer operation. These shutdown periods can be considered in the optimization problem through binary variables.¹² However, since this study deals with large-scale hydrogen production, the number of required stacks is sufficient to render the minimum load factor negligible. Thus, individually accounting for on–off periods is not required.

Compressor. Hydrogen compression is considered as a polytropic compression, as shown in eq 6.³⁹

$$P^{\text{Comp}} = \frac{\dot{m}_{\text{Comp}}^{\text{in}} \cdot RkT}{\text{MW} \cdot (k - 1) \cdot \eta_{\text{Comp}}} \left(\left(\frac{P_{\text{H}_2}}{P_{\text{el}}} \right)^{k-1/k} - 1 \right) \quad (6)$$

Here, the compressor power requirement is dependent on the hydrogen mass flow ($\dot{m}_{\text{Comp}}^{\text{in}}$), the compressor efficiency (η_{Comp}), the polytropic coefficient (k), the molecular weight of hydrogen (MW), and the ratio of out/in pressure ($\frac{P_{\text{H}_2}}{P_{\text{el}}}$) inside the vessel.

To allow for a linear equation to represent the compression stage, the pressure inside the vessel is considered constant and equal to the maximum pressure of the vessel;¹² then, eq 6 simplifies to eq 7.

$$\text{Power}_{t,d,r}^{\text{Comp}} = k_{\text{Compressor}} \cdot \dot{m}_{\text{AE},t,d,r}^{\text{out}} \quad (7)$$

where $k_{\text{Compressor}}$ brings together all the constant parameters in eq 6; $k_{\text{Compressor}}$ is set to $4 \left[\frac{\text{kW h}}{\text{kg H}_2} \right]$.¹²

Hydrogen Storage in Tanks. Analogous to energy storage in batteries, modeling hydrogen storage in tanks requires two equations: (i) mass balance to relate the level of storage, as shown in eq 8, where a discharge efficiency of 95% is considered to account for pumping or leakage losses,⁴⁰ and (ii) the maximum hydrogen level (HL) in the tank as a safety measure which is captured in eq 9; a value of 95% of the nominal capacity is considered in this study.

$$m_{t,d,r}^{\text{Acc}} = m_{t-1,d,r}^{\text{Acc}} + \Delta t \cdot \left(\dot{m}_{t-1,d,r}^{\text{in}} - \frac{\dot{m}_{t-1,d,r}^{\text{out}}}{\eta_{\text{tank}}} \right) \quad (8)$$

$$0 \leq m_{t,d,r}^{\text{Acc}} \leq \text{HTL}_{\max} \cdot \text{Cap}_{\text{tank},d,r} \quad (9)$$

Capacity Expansion Modeling. In this problem, any location is allowed to increase or decrease the installed capacity. We consider that due to the rapidly emerging green hydrogen industry in Chile, any expansion project requires a year-long development and that increments in capacity become available gradually at each trimester. The reduction in capacity is considered as the halt of operation, which is assumed to take the minimal day unit of the model, i.e., a trimester.

Equation 10 presents the model for technology capacity through the time horizon as a stock constraint.

$$\text{Cap}_{i,d,r} = \text{Cap}_{i,d-1,r} + \sum_{\hat{d}=d}^{d+2} \left(\frac{1}{3} \text{CapE}_{i,\hat{d}} \right) - \text{CapD}_{i,d-2,r} \quad (10)$$

In here, $\sum_{\hat{d}=d}^{d+2} \left(\frac{1}{3} \text{CapE}_{i,\hat{d}} \right)$ corresponds to the gradual increment in capacity in a trimester.

The system's capacity expansion and capacity reduction are, respectively, associated with binary variables $Y_{i,r,d}$ $X_{i,r,d}$ defined as

$$Y_{i,r,d} = 1 \quad \begin{array}{l} i \text{ starts a capacity expansion at day } d \\ \text{in location } r \end{array}$$

$$X_{i,r,d} = 1 \quad \begin{array}{l} i \text{ starts a capacity reduction at day } d \\ \text{in location } r \end{array}$$

If an expansion project is being developed for a technology at a specific location, then no other expansion or reduction project can be started for said technology at that location. These logical relations are presented in eq 11 (no simultaneous start of expansion and reduction projects); eq 12 (no further expansions if an expansion is undergoing) and eq 13 (no reduction if an expansion project is undergoing).

$$Y_{i,d,r} + X_{i,d,r} \leq 1 \quad (11)$$

$$\sum_{\hat{d}=d+1}^{d+2} Y_{i,\hat{d},r} \leq 2 \cdot (1 - Y_{i,d,r}) \quad (12)$$

$$\sum_{\hat{d}=d+1}^{d+2} X_{i,\hat{d},r} \leq 2 \cdot (1 - Y_{i,d,r}) \quad (13)$$

Upper-bound constraints are implemented to associate the existence of capacity-altering projects with the corresponding

magnitude of capacity expansion/reduction. Equations 14 and 15 show the said constraints.

$$\text{CapE}_{i,d,r} \leq \text{Max}_i \cdot Y_{i,d,r} \quad (14)$$

$$\text{CapD}_{i,d,r} \leq \text{Max}_i \cdot X_{i,d,r} \quad (15)$$

Objective Functions. Economic Objective Function. The economic objective function is presented in eq 16. Land acquisition, CAPEX, OPEX, H₂ opportunity cost, and a discount factor are considered for each region and are defined below.

$$\min : \text{Land} + \sum_{d \in D} \text{DF}_d \cdot (\text{CAPEX}_d + \text{OPEX}_d + C_{\text{Op}_d}^{\text{H}_2}) \quad (16)$$

Land Investment. We assume that the land is acquired during the first year for each location and that the total cost is linearly dependent on the purchased area, as stated in eq 17.

$$\text{Land} = \sum_{r \in R} C_r^{\text{Area}} \cdot A_r \quad (17)$$

CAPEX. Equations 18 and 19, respectively, present the capital expenses at the beginning of the time horizon (day 0) and those of subsequent capacity expansions. CAPEX includes the costs of equipment and installation of each technology, where said cost is expressed as $\frac{\text{USD}}{\text{kW}, \text{kg/h}, \text{kg or kW h}}$ depending on the equipment.

$$\text{CAPEX}_0 = \sum_{i \in I, r \in R} C_i^{\text{Impl}} \cdot \text{Cap}_{i,0,r} \quad (18)$$

$$\text{CAPEX}_{d \neq 0} = \sum_{i \in I, r \in R} C_i^{\text{Impl}} \cdot \text{CapE}_{i,d,r} \quad (19)$$

Following Corengia and Torres, 2022,¹² for this study, the installed capacity and capital cost are assumed to have a linear relation as electrolyzers of capacities larger than 2MW are expected and are currently built by stacking smaller units. No improvements in the technology or costs of each equipment were considered during the time horizon evaluated in the model, although we acknowledge they may happen.⁴¹

OPEX. OPEX is defined as operational and maintenance cost (O&M) and is considered a percentage of installed capacity (CAPEX); it is calculated, as shown in eq 20.

$$\text{OPEX}_d = \sum_{i \in I, r \in R} C_i^{\text{Op}} \cdot C_i^{\text{Impl}} \cdot \text{Cap}_{i,d,r} \quad (20)$$

Here, the parameter C_i^{Op} corresponds to the O&M costs of each trimester associated with the installed capacity.

H₂ Opportunity Cost. In this study, we refer to H₂ opportunity cost as the loss of potential income related to the decision of storing H₂ instead of selling it to the market. Including this opportunity cost prevents the system from increasing resilience by overstoring H₂. We model this opportunity cost, as shown in eq 21.

$$C_{\text{H}_2,d}^{\text{Op}} = P_{\text{H}_2}^{\text{Sale}} \cdot \sum_{t \in T, r \in R} m_{t,d,r}^{\text{Acc}} \quad (21)$$

It is important to note that stored energy does not have an opportunity cost since the proposed plants are assumed to be off-grid, and hence, it is not possible to directly sell the stored energy.

Discount Factor. A discount factor is considered for the CAPEX, the OPEX, and the H₂ opportunity cost to account for

the time value of money. Equation 22 exhibits the discount factor for a given interest rate r .

$$\text{DF}_d = \frac{1}{(1+r)^d} \quad (22)$$

The discount factor of the last representative day is modified, as shown in eq 23. Here, a perpetuity is considered for any capacity still in place at the end of the time horizon. This perpetuity ensures that capacity spikes will not occur near the end of the time horizon due to less-relevant present cost values.⁴²

$$\text{DF}_{d_f} = \frac{1}{(1+r)^{d_f}} + \frac{1}{(1+r)^{d_f+1}} \cdot \frac{1}{\left(1 - \frac{1}{(1+r)}\right)} \quad (23)$$

Resilience Objective Function. In this study, a system will be considered operationally resilient if it has sufficient autonomy to withstand noncatastrophic unfortunate events. Such events are variations of RE sources (exogenous) and internal plant operation failure (endogenous). Both of these events could cause a deficit in hydrogen production, either by a shortage of energy or by the unavailability of operational capacity.

We will use the term heteronomy to refer to the lack of autonomy of the system due to its dependence on conditions that the system cannot manage.

We consider two essential distinctions of unfortunate events that an autonomous system must endure: (i) external events associated with the intrinsic unpredictable behavior that REs have and its effect on the operation of a plant designed through statistical averages of representative days and (ii) internal events, associated with specific failures in the normal plant operation and its corresponding negative effect in production.

Modeling External Variability. The model must acknowledge that the parameters of solar radiation and wind speed used for the sizing of generators of renewable electricity are averages and are subject to variation. In this sense, locations with favorable average solar radiation or wind speed might have a high variance, which is not a desired attribute for an off-grid hydrogen plant.

This variability is dependent on the installed area of renewable sources at each location, the day, and hour of said day, as shown in eqs 24 and 25.

$$\text{Var}_{\text{PV},t,d,r} = \eta_{\text{PV}} \cdot A_{d,r}^{\text{PV}} \cdot \sigma_{\text{PV},t,d,r} \quad (24)$$

$$\text{Var}_{\text{Wind},t,d,r} = \frac{1}{2} \cdot C_{\text{Wind}} \cdot A_{d,r}^{\text{Wind}} \cdot \rho_{\text{Air}} \cdot (\sigma_{\text{Wind},t,d,r})^3 \quad (25)$$

Here, $\sigma_{\text{PV},t,d,r}$ and $\sigma_{\text{Wind},t,d,r}$ correspond to the historical deviations of solar radiation and wind speed on an hourly basis for each trimester and each location, respectively. The overall variability

${}^{\text{ext}}\delta E_{t,d,r}^-$ is the sum of both sources

$${}^{\text{ext}}\delta E_{t,d,r}^- = \sum_{e \in \text{RE}} \cdot \text{Var}_{e,t,d,r} \quad (26)$$

A deficit of energy from renewable sources ultimately results in a deficit in hydrogen production since not all of the required power will be supplied to the electrolyzer. The system can compensate for this deficit with storage, which can be either in the form of energy in the battery system ([kW h]), which will supply power to the electrolyzer, or as hydrogen itself in tanks ([kg]). The availability of storage can then be calculated, as shown in eq 27, where

$$\text{Storage}_{t,d,r} = \eta_{\text{Discharge}} \cdot E_{t,d,r}^{\text{Acc}} + \frac{m_{t,d,r}^{\text{Acc}}}{\eta_{\text{AE}}} \quad (27)$$

The net deficit in production due to external variance is then defined as the difference between the expected RE source-induced variability and the compensation that might be achieved by the storage systems. [Equation 28](#) shows the mathematical representation of said term. ER

$${}^{\text{ext}}\Delta E_{t,d,r}^- = {}^{\text{ext}}\delta E_{t,d,r}^- - \text{Storage}_{t,d,r} \quad (28)$$

Note that if the net externally induced variability ${}^{\text{ext}}\Delta E_{t,d,r}^-$ is greater than 0, then the system does not have sufficient storage to withstand the variance of the renewable sources.

Modeling Internal Variability. According to Peyghami et al.,⁴³ one of the pieces of equipment most prone to fail in a power system are converters, including DC boosters and rectifiers. [Figure 1](#) exhibits where said converters are located in the architecture of the plant's electrical system. Internal variability will consider the availability of renewable sources and the electrolyzer based on their associated converters. Since the availability parameter will vary with the converter circuit architecture,⁴³ this study will refer to accepted literature values for solar PV panels and wind turbines of 96%.⁴⁴ DC boosters for AE circuit designs are still being developed,⁴⁵ and a 90% availability is assumed.

As shown in [Figure 1](#), failure in the renewable source generators will result in a deficit of energy (δE^-). Meanwhile, failure of the electrolyzer will result in a deficit in the associated flow of hydrogen (δM^-). [Equations 29](#) and [30](#), respectively, characterize said energy and mass deficit as a function of the installed capacity ($\text{Cap}_{i,d,r}$)

$${}^{\text{int}}\delta E_{d,r}^- = \sum_{e \in \text{RE}} (1 - \Lambda_e) \cdot \text{Cap}_{e,d,r} \quad (29)$$

$${}^{\text{int}}\delta M_{d,r}^- = (1 - \Lambda_{\text{AE}}) \cdot \text{Cap}_{\text{AE},d,r} \quad (30)$$

where Λ_e and Λ_{AE} represent the availability coefficient of the renewable sources and the alkaline electrolyzer, respectively.

As previously stated, the storage system may compensate for the said variability. In this case, the battery system can only compensate if the failure is in the RE generators ([eq 31](#)), while a failure in the electrolyzer can only be compensated by storage of hydrogen in tanks ([eq 32](#)).

$${}^{\text{int}}\Delta E_{t,d,r}^- = {}^{\text{int}}\delta E_{d,r}^- - \eta_{\text{Disch}} \cdot E_{t,d,r}^{\text{Acc}} \quad (31)$$

$${}^{\text{int}}\Delta M_{t,d,r}^- = {}^{\text{int}}\delta M_{d,r}^- - m_{t,d,r}^{\text{Acc}} \quad (32)$$

Proposed Objective Function for Resilience. The objective function for minimizing the net variability in the system is defined as the combination of the equations discussed above. Hence

$$f_{\text{heteronomy}} = \sum_{t,d,r} \eta_{\text{AE}} \cdot ({}^{\text{int}}\Delta E_{t,d,r}^- + {}^{\text{ext}}\Delta E_{t,d,r}^-) + {}^{\text{int}}\Delta M_{t,d,r}^- \quad (33)$$

This expression can be interpreted as the system heteronomy; its sign will determine if the design can overcome the external and internal variance with its storage capacity. Hence, a negative value indicates that storage is larger than the variance and thus adequately overcomes failures. A positive value, on the other hand, indicates that storage cannot adequately overcome the

failures. In this sense, an optimally resilient system can be defined as one with a minimal heteronomy.

CASE STUDY

We evaluate the production of green hydrogen in five locations of the Biobío region in Chile, namely: Negrete, Aguapie, Lavapie, Rumena, and Colhue. The Biobío region presents favorable sun radiation and wind speed; the mentioned locations are chosen based on data availability in terms of area and climatic condition data availability. Specific data were obtained from the Chilean wind⁴⁶ and solar observatories.⁴⁷

In terms of demand, this study will consider the work by Lane et al.,⁴⁸ which forecasts the demand for renewable hydrogen at a global scale using Monte Carlo simulations to incorporate uncertainty and a learning curve. Providing the demand scenarios are shown in [Figure 3](#). To assess the model, we

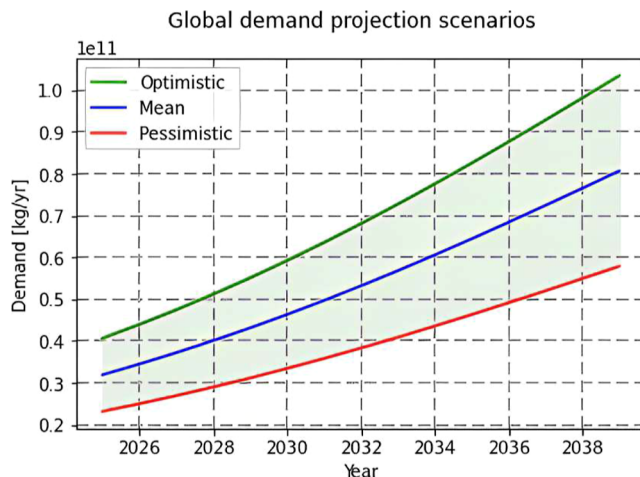


Figure 3. Global hydrogen demand projection through a learning curve for pessimistic, normal, and optimistic scenarios.

further assume that Chile plans to supply 20% of the global hydrogen demand and the Biobío region 1% of the total Chilean production. This provides a feasible regional demand for the case study, involving production in all different locations. The values extracted for demand,⁴⁸ location costs, and available area according to the SII database,⁴⁹ and other parameters are present in the [Supporting Information](#).

RESULTS

The model for the case study in the previous section was implemented in PyOMO^{50,51} and solved using the Gurobi MILP solver⁵² on a regular portable laptop. The model constitutes a total of 82,811 variables, where 2705 variables are binary and 80,106 are continuous, related through 50,025 equality and 51,745 inequality constraints. The MIP gap terminal condition is maintained at its default value of 1×10^{-4} .

Single-Objective Solutions and Multiplicity Analysis. Being a MILP problem, it is possible to achieve the same value of the objective function with different values for the arguments, and due to the MIP gap termination condition, a more thorough search might obtain better solutions. To evaluate the optimal design, successive integer cuts were implemented to obtain three alternate solutions. [Equation 34](#) shows the “no good cut”, where the variable $z_{i,d,r}$ represents the expansion ($X_{i,d,r}$) and decrease ($Y_{i,d,r}$) binary choices; B and NB are the set of basic and nonbasic solutions, respectively.

$$\sum_{i,d,r \in NB} z_{i,d,r} + \sum_{i,d,r \in B} (1 - z_{i,d,r}) \geq 1 \quad (34)$$

Table 1 shows the alternative optima (after integer cuts) for the single-objective models, i.e., those solutions in which the

Table 1. Optimal Value for the Objective Functions in Each Single-Objective Model^a

solution	model	
	economic [USD]	heteronomic [kg]
optimal value	1.5996×10^9	-9.4439×10^9
Objective Value Difference (%)		
alternative #1	0	$\approx 2.8 \times 10^{-5}$
alternative #2	0	$\approx 2.5 \times 10^{-5}$
alternative #3	$\approx 2.8 \times 10^{-4}$	$\approx 2.2 \times 10^{-5}$

^aAlternate solutions' values are presented as a difference from the optimal solution objective.

weights for combining the economic and heteronomy objective functions were either 0 (purely resilient objective) or 1 (purely economic objective). These solutions are termed alternatives in the table. The purely economic single-objective model presents 2 alternative solutions with the same value for the objective function. Meanwhile, no equivalent solutions were found for the pure heteronomy single-objective model; three other alternative solutions were found with negligible differences in the value of the objective function. The differences in the expansion profiles for the alternate solutions are presented in the *Supporting Information*, where only a difference in the stored hydrogen at the end of the time horizon and in some expansion rates is observed in these cases. For the rest of the discussion, the results labeled as optimal value in **Table 1** are considered.

Multiobjective Solution—Pareto Optimal Results. Here, the problem was solved to find the Pareto frontier for the economic and heteronomous objective functions via the weighted sum method. A computation time of 4545 s was required to obtain the multiobjective Pareto frontier.

Figure 4a exhibits the Pareto curve and the equilibrium price of hydrogen, defined as the value required to achieve a zero net present value (*NPV*) for the plant investment and production costs. As expected, there is a trade-off between both objective functions, which relates to the fact that designing a more resilient

system requires more investment in storage technologies, directly raising the total cost and the equilibrium price for hydrogen. It is important to note that the heteronomy objective function has, at almost all points of the Pareto curve, a negative value. This implies that in almost all solutions, the designed network has enough storage to withstand the expected external and internal losses.

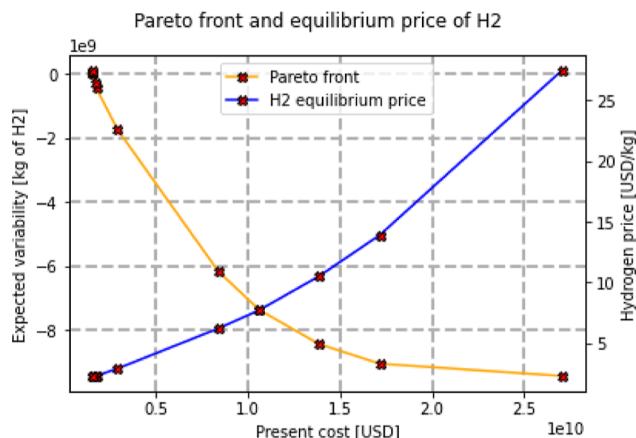
Figure 4b shows the equilibrium price for hydrogen versus the weight values for each point in the Pareto curve. The green region above the curve corresponds to the hydrogen prices that provide an economically feasible result (positive *NPV*). Inversely, the red region corresponds to hydrogen prices that make the system economically unfeasible.

In the following section, a weight of 0.6, associated with a hydrogen equilibrium price of $2.3 \left[\frac{\text{USD}}{\text{kg H}_2} \right]$, is selected as the desired solution from the Pareto frontier and will be referred as the autonomy-enhanced solution. This equilibrium price is lower than the $2.6 \left[\frac{\text{USD}}{\text{kg H}_2} \right]$ benchmark established by the Chilean national hydrogen plan for the Biobío region,⁵⁴ in addition to presenting a negative heteronomy value. A similar analysis for other weights could be performed if desired.

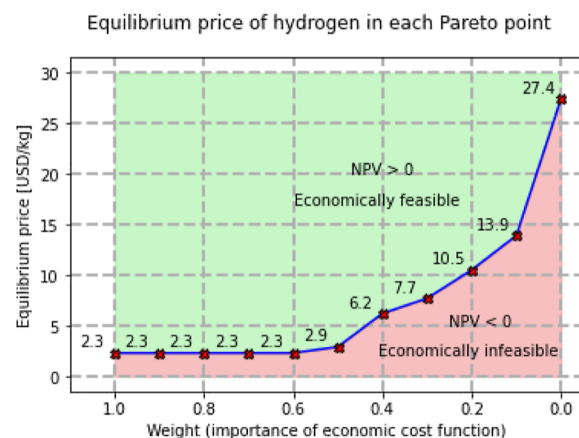
Summary of System Design. **Table 2** summarizes key changes in the design of HRES systems for green hydrogen production when the economic objective function model is enhanced with consideration of heteronomy.

Compared to the economic model, no relevant changes in the start years of each location are seen, where Negrete and Aguapie start in 2025 and the rest in 2026. In all cases, a hybrid power system (wind and solar) is selected. Comparing the autonomy-enhanced and the economic solution, generation from wind energy sources is implemented at a lower magnitude in Lavapie, Aguapie, and Colhue, followed by an increase in solar capacity for the said locations. However, the change is substantial only for Lavapie.

As expected, the most relevant difference between the two objectives is related to storage. Battery storage is not installed at Negrete and Colhue when only the economic function is considered; in contrast, the autonomy-enhanced solution increases the energy storage capacity in batteries for each location. Hydrogen storage in tanks also follows the tendency of



(a) Pareto front and equilibrium price of H_2



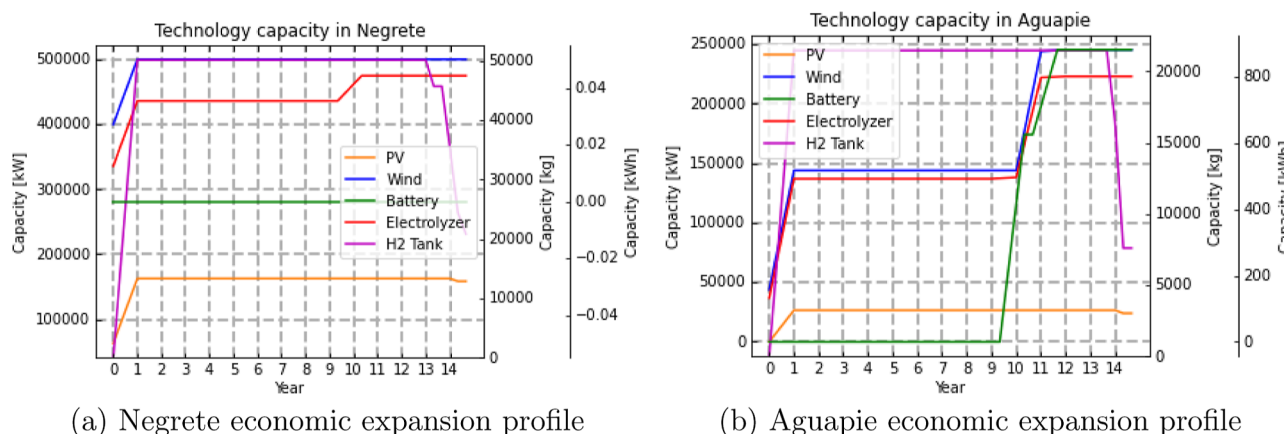
(b) H_2 equilibrium price in the Pareto front.

Figure 4. Pareto frontier and hydrogen equilibrium price.

Table 2. Results Overview for the Single-Objective and Autonomy-Enhanced Solutions^a

result	model	Rumena	Negrete	Aguapie	Lavapie	Colhue
starting year	economic	2026	2025	2025	2026	2026
	enhanced	2026	2025	2025	2026	2026
solar source capacity [MW]	economic	[0–14]	[63–162]	[0–26]	[0–22]	[0–25]
	enhanced	[0–16]	[61–161]	[0–32]	[0–24]	[0–27]
wind source capacity [MW]	economic	[0–109]	[400–500]	[44–245]	[0–167]	[0–205]
	enhanced	[0–109]	[400–500]	[44–239]	[0–161]	[0–100]
battery capacity [MWh]	economic	[0 ₍₁₎ –2.1]	0	[0 ₍₉₎ –0.8]	[0 ₍₁₁₎ –4.4]	0
	enhanced	[0 ₍₉₎ –5.3]	[0–5.9]	[0–4.6]	[0–7.7]	[0–0.7]
H ₂ storage capacity [ton]	economic	[0–10]	[0–50]	[0–21]	[0–14]	[0–16]
	enhanced	[1–100]	[0–100]	[0–100]	[0–100]	[0–100]
H ₂ equilibrium price [USD/kg]	economic	\$ 2.3			enhanced	
					\$ 2.3	

^aCapacities are presented as intervals of the minimal and maximum values in the time horizon, expressed as [min–max]. Zero values that have an index *n* refer to the number of years (*n*) that the capacity value remains at 0. If *n* < 1 year, no index is implemented.

**Figure 5.** Expansion profiles of the economic model for Negrete (a) and Aguapie (b), respectively.

higher capacities when the heteronomy of the system is considered, increasing to 100 t at each location.

It is important to note that the implementation of these storage technologies comes without a noticeable increase in the equilibrium price of hydrogen; for the selected economic/heteronomy combined solution, an investment of 0.37 [USD] is required per kilogram of H₂ mass variability reduction.

Analyzing the Pareto frontier and how the optimal point shows a considerable increase in present cost, useful remarks arise for future studies: Figure 4a shows that most Pareto points have more than enough mass and energy storage to withstand the accounted variability and that the spike in cost is associated with the said increase in storage capacity. Diminishing the value of the upper bound in the constraint associated with storage technologies' capacity, specifically mass storage, provides a system design with less-idle storage, reducing the overall cost of each point in the Pareto frontier and managing a less-considerable cost compared to the economic model. A 75% reduction in the upper bound is analyzed through the Pareto optimal hydrogen equilibrium prices, resulting in an increase in the economically feasible region due to lower equilibrium prices throughout the Pareto front (Supporting Information).

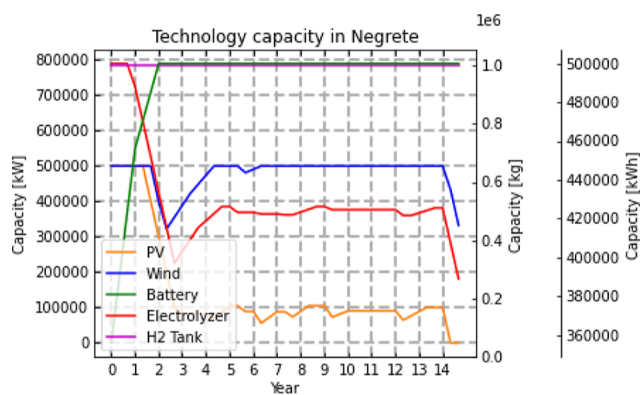
Capacity Expansion: Single-Objective and Autonomy-Enhanced Solution Comparison. In this section, the different system designs are compared for the single-objective models and the enhancement of incorporating the multi-objective approach. The capacities of each technology are analyzed for the locations of Negrete and Aguapie, exposing the

effects of the proposed heteronomic objective function in the design of the system.

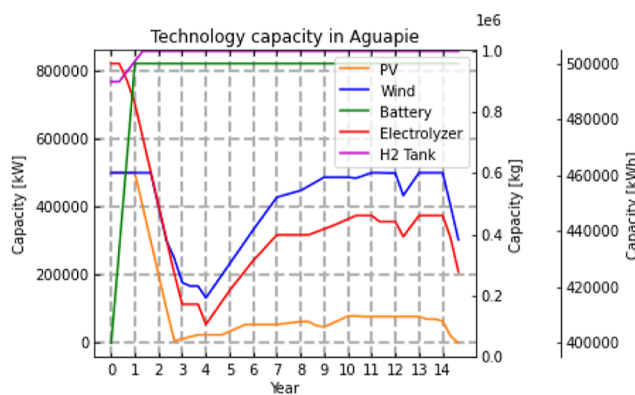
Figure 5 shows the expansion profiles for the economic single-objective model in the mentioned regions. In both locations, hydrogen storage and a hybrid power system of solar and wind for the complete time horizon are obtained as the optimal design. In Negrete, the installation of energy sources and hydrogen storage is completed by the 1st year, and an expansion of the electrolyzer capacity is implemented in the 9th year of operation. Meanwhile, Aguapie completes the installation of hydrogen storage and solar energy generators in the 1st year of implementation, and an expansion between the 9th and 11th year for the wind energy generators, electrolyzer, and battery system is considered.

Neither location considers a battery system for the first 9 years of operation, and Negrete does not implement a battery system. The preference for a hydrogen storage system is related to the more cost-efficient hydrogen mass storage over the lithium ion batteries for long periods since the latter have passive losses and present a higher maintenance cost. Because of this, hydrogen storage is preferred over energy storage, even when an opportunity cost for hydrogen is implemented.

In both locations, a decrease in the hydrogen storage capacity starts from the 13th year until the end of the time horizon to avoid the perpetuity cost effects, where it is cheaper to diminish hydrogen storage and fulfill demand with production and dispatch the already available stored hydrogen.

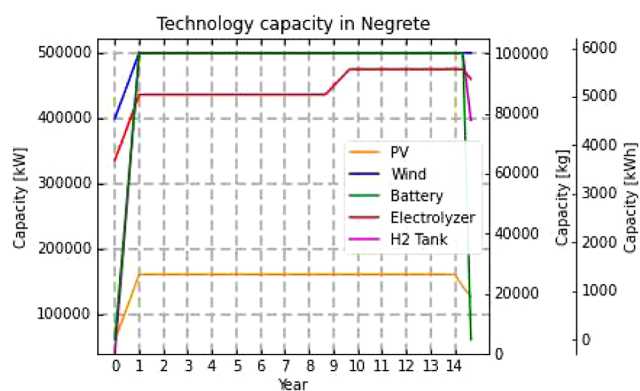


(a) Negrete heteronomic expansion profile

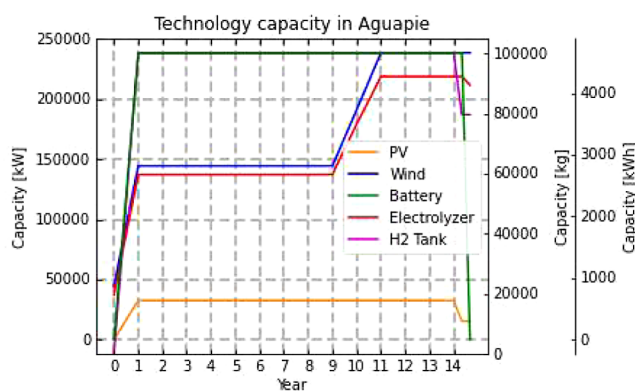


(b) Aguapie heteronomic expansion profile

Figure 6. Expansion profiles of the heteronomy model for Negrete (a) and Aguapie (b), respectively.

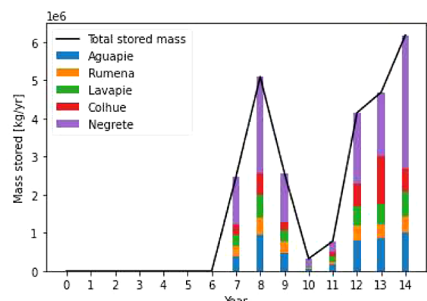


(a) Negrete autonomy enhanced expansion

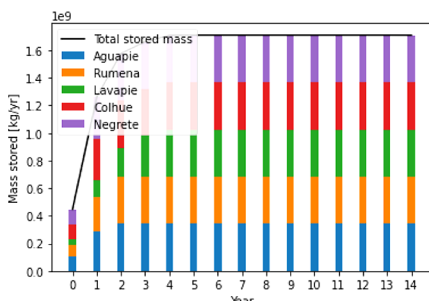


(b) Aguapie autonomy enhanced expansion

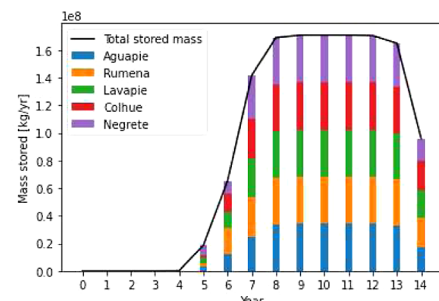
Figure 7. Expansion profiles of the autonomy-enhanced solution for Negrete (a) and Aguapie (b), respectively.



(a) Economic model hydrogen storage profile.



(b) Heteronomy model hydrogen storage profile.



(c) Autonomy enhanced hydrogen storage profile.

Figure 8. Hydrogen storage profile for the single and autonomy-enhanced solutions.

Figure 6 shows the expansion profiles for the heteronomic single-objective model in Negrete and Aguapie, respectively. Both locations present similar profiles, with the installation of both hydrogen and energy storage systems at maximum capacity for the complete time horizon. A hybrid power system dominated by wind energy is present for each location as well, with a reduction in the generation capacity of the RE sources and electrolyzer until the 3rd and 4th year, when a subsequent expansion is implemented.

The increase of the storage technologies' capacity is associated with the objective function formulation as more storage implies a reduced dependence on external and internal

variability. The reduction in RE source generation and electrolyzer capacities seeks to minimize the variability of the system since a larger installed capacity results in larger internal and external expected variability. Therefore, the heteronomous model maximizes storage capacity while maintaining a minimum required energy source and electrolyzer capacity.

Figure 7 shows the expansion profiles for the autonomy-enhanced solution in Negrete and Aguapie, respectively. For both locations, a wind-dominated hybrid power system with dual-storage technologies is implemented. In Negrete, the installation of the power generation, the battery system, and the hydrogen storage was complete in the 1st year of implementa-

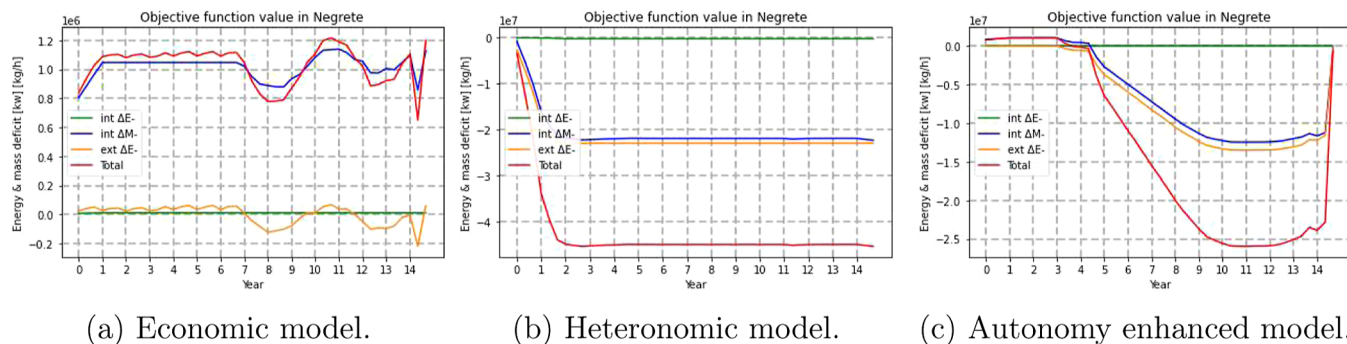


Figure 9. Heteronomy objective function behavior for the economic, heteronomic, and autonomy-enhanced models.

tion. Aguapie's battery system, hydrogen storage, and power generation from solar energy are fully implemented by the 1st year, whereas power generation from wind and electrolyzer capacity have an expansion in the 9th year of operation. Both locations present a reduction in capacity in the last 2 years of the time horizon, associated with the perpetuity effects of the economic objective function.

Compared with the purely economic objective, the results show that adding the heteronomy function in a multiobjective approach impacts the system design, promoting dual storage throughout the complete time horizon. The magnitude of the change varies: hydrogen storage increased its maximum value from 50 [ton] in the economic model to 100 [ton] in the autonomy-enhanced solution in Negrete and from 21 to 100 [ton] in Aguapie. Energy storage also increased compared to the economic model, from 800 to 4600 kW h in Aguapie and from 0 to 5900 kW h in Negrete. A slight increase in the solar power capacity is also perceived in Aguapie.

Role and Effects of Hydrogen Storage. Figure 8 shows the mass of hydrogen stored in each location throughout the years for the economic, heteronomy-, and autonomy-enhanced solutions.

As seen, the economic model has a null storage of H_2 mass in the first 6 years, presenting peaks before and after the 10 years of operation. The first peak (8th year) is related to the capacity expansion profiles present in Figures 5a,b. The 10th year of the horizon is when most of the system increases its capacity, and since this requires a year to accomplish, the network must have enough storage to fulfill the increase in demand associated with that year beforehand. The second increment after the 10th year relates to the end-of-time effects in the economic objective function since the system stores hydrogen to fulfill demand in the last year of operation. The heteronomy model increases storage rapidly, reaching a constant value by the 3rd year (see Figure 8b) since, as expected, the purely heteronomy-based model maximizes storage to overcome disruptions. The autonomy-enhanced solution encompasses the characteristics of both models.

The effects of these different storage profiles in the resilience of the system can be addressed through the value of the heteronomy function since it measures how much autonomy the designed system has. As an example, Figure 9 exhibits these values for the Aguapie region. Other locations present analogous behaviors.

Figure 9a shows that the total heteronomy value of the economic model design is positive throughout the complete time horizon. This is evidence that the designed system lacks autonomy and would be vulnerable to the exogenous variability

of the RE sources and endogenous component failure. Hence, the role of storage as a tool for expansion in the economic model does not bring operational resilience to the design. In contrast, the autonomy-enhanced solution presents a positive value of heteronomy for the first 5 years and a negative value for the rest of the horizon. This indicates that the multiobjective approach manages to design a storage system that can provide sufficient autonomy to the system for the majority of the time horizon.

The higher installation of storage capacity, the increase of total stored mass, and the objective function behavior shown in Figure 9 shows that, without a relevant increase in the hydrogen equilibrium price, the incorporation of the heteronomy function to the multiobjective optimization manages to design a system that is more autonomous in front of exogenous and endogenous effects than a purely economic model.

CONCLUSIONS

A multiobjective mixed integer linear programming model was developed as a decision-making tool to analyze green hydrogen production at a regional level. The tool introduces a novel resilience objective function that minimizes the variability of the system by designing a hybrid storage system capable of mitigating the fluctuations intrinsic to RE sources as well as internal plant failures, striving for simplicity and reasonable computational resource use.

As a case study, the program considers the production of green hydrogen in five regions of Chile that differ in their climate conditions and land cost. In all cases, the optimal resilient system design is a hybrid dual-storage system, where wind power is the dominant energy source.

The optimal designs incorporate storage technologies with a capacity larger than the most economical one, covering the estimated deficit in hydrogen and electricity with a sufficient surplus throughout most of the time horizon. Considering the five regions, the investment cost of H_2 mass variability reduction

is about $0.37 \left[\frac{\text{USD}}{\text{kg } H_2} \right]$ between the purely economically optimal model and the autonomy enhanced one. Even when considering the addition of battery systems at higher capacities over the time horizon, the hydrogen equilibrium price does not vary considerably, remaining at 2.3 [USD/kg], which is lower than the 2.6 [USD/kg] projected by the Chilean hydrogen strategy. Hence, the incorporation of a hybrid battery/hydrogen storage system provides a benefit to the system's autonomy without affecting the overall cost.

This study's methodology may be implemented to on-grid hydrogen system designs by the addition of relevant components for power grid modeling, such as transmission,

generation, ramping rates, and demand fulfillment. Future studies may complement this approach by implementing different time aggregation techniques and representative day selection strategies to analyze the role of data representability for the applied case studies. This research methodology approach can be implemented in other power-to-X off-grid systems for a more diverse regional design, considering the storage/cost trade-off in a manageable manner. Furthermore, it can be extended to other disciplines after properly reinterpreting the terms.

ASSOCIATED CONTENT

Supporting Information

The Supporting Information is available free of charge at <https://pubs.acs.org/doi/10.1021/acs.iecr.3c03060>.

Condensed formulation: complete formulation of the MILP problem; parameters for the case study: parameters used in the case study, hydrogen demand projection according to the literature, and the electrolysis technologies' cost comparison; complementary results: results mentioned in the text, corresponding to alternative designs after the implementation of integer cuts, and the storage capacity constraint effects in equilibrium prices; and representative day selection: additional information regarding the representative days chosen for the case study ([PDF](#))

AUTHOR INFORMATION

Corresponding Author

Felipe A. Díaz-Alvarado – Department of Chemical Engineering, Biotechnology, and Materials, Faculty of Physical and Mathematical Sciences, Universidad de Chile, Santiago 8370456, Chile;  orcid.org/0000-0002-2182-790X; Email: felidiaz@ing.uchile.cl

Authors

Andrés I. Cárdenas – Department of Chemical Engineering, Biotechnology, and Materials, Faculty of Physical and Mathematical Sciences, Universidad de Chile, Santiago 8370456, Chile;  orcid.org/0009-0008-4423-4104

Ana Ines Torres – Department of Chemical Engineering, Carnegie Mellon University, Pittsburgh, Pennsylvania 15213, United States

Complete contact information is available at:

<https://pubs.acs.org/10.1021/acs.iecr.3c03060>

Notes

The authors declare no competing financial interest.

ACKNOWLEDGMENTS

Ana I. Torres thanks for the start-up funds from Carnegie Mellon University. Felipe Díaz-Alvarado and Andrés I. Cárdenas thank the support from Enlace Fondecyt project from Universidad de Chile.

NOMENCLATURE

Indexes

- d representative day
- e renewable energy source
- i technology (superstructure equipment)
- r location
- t time of day

Parameters

ΔH_{PV}	hydrogen electrolysis reaction enthalpy
η_{Charge}	solar panel efficiency
$\eta_{\text{Discharge}}$	battery charge efficiency
η_{Tank}	battery discharge efficiency
λ	hydrogen tank discharge efficiency
Λ_i	wind turbine swipe area to land usage ratio
ρ_{Air}	availability of technology i
$A_{r,\text{Max}}$	air density
C_i^{Impl}	maximum available area in location r
C_i^{Op}	implementation cost of technology i
C_p^{Wind}	O&M cost of technology i
Demand_d	wind turbine capacity factor
$G_{t,d,r}^{\text{Sun}}$	hydrogen demand for day d (trimester demand)
HTL_{Max}	average solar radiation at time t at day d in location r
$k_{\text{Compressor}}$	maximum hydrogen level in the hydrogen tank system
L_{Battery}	compressors power consumption constant
M	battery passive losses
$P_{\text{H}_2}^{\text{Sale}}$	a sufficiently large number
$\text{SOC}_{\text{Min},\text{Max}}$	hydrogen selling price
η_{AE}	minimal and maximal states of charge for the battery system
	alkaline electrolyzer efficiency

Supplementary Definitions

${}^{\text{ext}}\Delta E_{t,d,r}$	net energy variability from external influences at time t at day d in location r
${}^{\text{ext}}\delta E_{t,d,r}$	overall energy variability from external influences at time t at day d in location r
${}^{\text{int}}\Delta E_{t,d,r}$	net energy variability from internal influences at time t at day d in location r
${}^{\text{int}}\delta E_{t,d,r}$	overall energy variability from internal influences at time t at day d in location r
${}^{\text{int}}\Delta M_{t,d,r}$	net mass variability from internal influences at time t at day d in location r
${}^{\text{int}}\delta M_{t,d,r}$	overall mass variability from internal influences at time t at day d in location r
CAPEX_d	implementation cost at day d
DF_d	discount factor at day d
Land	total land acquisition cost
OPEX_d	operational cost at day d
$\text{Storage}_{t,d,r}$	available storage at time t at day d in location r
$\text{Var}_{e,t,d,r}$	installed variability associated with source e at time t at day d in location r
$C_{\text{Op},d}^{\text{H}_2}$	stored hydrogen opportunity cost at day d

Variables

$\dot{E}_{e,t,d,r}^{\text{Direct}}$	energy flow directed to the AE from source e at time t at day d in location r
$\dot{E}_{e,t,d,r}^{\text{Storage}}$	energy flow directed to the battery storage from source e at time t at day d in location r
$\dot{m}_{t,d,r}^d$	mass flows supplied to demand directly from the AE at time t at day d in location r
$\dot{m}_{t,d,r}^{\text{out}}$	outgoing mass flow from the AE at time t at day d in location r
$A_{d,r}^{\text{PV}}$	installed pv panel area at day d in location r
$A_{d,r}^{\text{Wind}}$	installed wind turbine swipe area at day d in location r
A_r	bought land in location r
$\text{Cap}_{i,d,r}$	capacity of technology i at day d in location r
$\text{CapD}_{i,d,r}$	amount of capacity downgrade for technology i at day d in location r

$\text{CapE}_{i,d,r}$	amount of capacity expansion for technology i at day d in location r
H_r	one if location r is used in the regional production
$\text{Power}_{i,d,r}^{\text{Comp}}$	compressor power consumption at time t at day d in location r
$X_{i,d,r}$	one if a decrease for technology i starts at day d in location r
$Y_{i,d,r}$	one if an expansion for technology i starts at day d in location r
$\dot{E}_{\text{AE},t,d,r}^{\text{in}}$	total energy flow entering the AE at time t at day d in location r
$\dot{E}_{s,t,d,r}^{\text{in}}$	energy flow directed to battery storage at time t at day d in location r
$\dot{E}_{s,t,d,r}^{\text{out}}$	energy flow directed to the AE from the battery storage at time t at day d in location r
$\dot{m}_{s,t,d,r}^{\text{in}}$	mass flow supplied to the hydrogen tank at time t at day d in location r
$\dot{m}_{s,t,d,r}^{\text{in}}$	mass flow supplied to demand from the hydrogen tank at time t at day d in location r
$E_{t,d,r}^{\text{Acc}}$	energy stored in the battery system at time t at day d in location r
$m_{t,d,r}^{\text{Acc}}$	mass stored in the hydrogen tanks at time t at day d in location r

■ REFERENCES

- Olabi, A.; Abdelkareem, M. A. Renewable energy and climate change. *Renewable Sustainable Energy Rev.* **2022**, *158*, 112111.
- Maradin, D. Advantages And Disadvantages Of Renewable Energy Sources Utilization. *Int. J. Energy Econ. Policy* **2021**, *11*, 176–183.
- Swati Negi, L. M. Hybrid Renewable Energy System: A Review. *Int. J. Electron. Electr. Eng.* **2014**, *7*, 535–542.
- Kombargi, D. R.; Elborai, D. S.; Anouti, D. Y.; Hage, R.. The dawn of green hydrogen; Technical Report; Strategy, 2021;1116. <https://www.strategyand.pwc.com/m1/en/reports/2020/the-dawn-of-green-hydrogen/the-dawn-of-green-hydrogen.pdf>.
- Hammer, L.; Veith, E. *Hybrid Renewable Energy System Optimization Is Lacking Consideration of System Resilience and Robustness: An Overview*, 2021.
- Siddaiah, R.; Saini, R. A review on planning, configurations, modeling and optimization techniques of hybrid renewable energy systems for off grid applications. *Renewable Sustainable Energy Rev.* **2016**, *58*, 376–396.
- Lara, C. L.; Mallapragada, D. S.; Papageorgiou, D. J.; Venkatesh, A.; Grossmann, I. E. Deterministic electric power infrastructure planning: Mixed-integer programming model and nested decomposition solution algorithm. *Eur. J. Oper. Res.* **2018**, *271*, 1037–1054.
- Alraddadi, M.; J Conejo, A.; M Lima, R. Expansion Planning for Renewable Integration in Power System of Regions with Very High Solar Irradiation. *J. Mod. Power Syst. Clean Energy* **2021**, *9*, 485–494.
- Wang, J.; Chen, H.; Cao, Y.; Wang, C.; Li, J. An integrated optimization framework for regional energy planning with a sustainability assessment model. *Sustain. Prod. Consum.* **2023**, *36*, 526–539.
- Cho, S.; Tovar-Facio, J.; Grossmann, I. E. Disjunctive optimization model and algorithm for long-term capacity expansion planning of reliable power generation systems. *Comput. Chem. Eng.* **2023**, *174*, 108243.
- Zhang, Q.; Martín, M.; Grossmann, I. E. *Computer Aided Chemical Engineering*; Elsevier, 2017; pp 1879–1884.
- Corengia, M.; Torres, A. I. Coupling time varying power sources to production of green-hydrogen: A superstructure based approach for technology selection and optimal design. *Chem. Eng. Res. Des.* **2022**, *183*, 235–249.
- Cooper, N.; Horrend, C.; Röben, F.; Bardow, A.; Shah, N. A framework for the design & operation of a large-scale wind-powered hydrogen electrolyzer hub. *Int. J. Hydrogen Energy* **2022**, *47*, 8671–8686.
- Gasser, P.; Lustenberger, P.; Cinelli, M.; Kim, W.; Spada, M.; Burgherr, P.; Hirschberg, S.; Stojadinovic, B.; Sun, T. Y. A review on resilience assessment of energy systems. *Sustain. Resilient Infrastruct.* **2021**, *6*, 273–299.
- Bruneau, M.; Chang, S. E.; Eguchi, R. T.; Lee, G. C.; O'Rourke, T. D.; Reinhorn, A. M.; Shinozuka, M.; Tierney, K.; Wallace, W. A.; von Winterfeldt, D. A Framework to Quantitatively Assess and Enhance the Seismic Resilience of Communities. *Earthq. Spectra* **2003**, *19*, 733–752.
- Francis, R.; Bekera, B. A metric and frameworks for resilience analysis of engineered and infrastructure systems. *Reliab. Eng. Syst. Saf.* **2014**, *121*, 90–103.
- Jackson, S.; Ferris, T. L. J. Resilience principles for engineered systems. *Syst. Eng.* **2013**, *16*, 152–164.
- Haimes, Y. Y.; Crowther, K.; Horowitz, B. M. Homeland security preparedness: Balancing protection with resilience in emergent systems. *Syst. Eng.* **2008**, *11*, 287–308.
- National Academy of Sciences. *Disaster Resilience: A National Imperative*; The National Academies Press, 2012.
- Heinimann, H. R.; Hatfield, K. *NATO Science for Peace and Security Series C: Environmental Security*; Springer Netherlands, 2017, pp 147–187.
- Vera, G. *Development of a Method for Planning a Resilient Multi-Vector Energy System through a Multi-Objective Optimization Model*, 2020.
- Rose, A. Economic resilience to natural and man-made disasters: Multidisciplinary origins and contextual dimensions. *Environ. Hazards* **2007**, *7*, 383–398.
- Omer, M.; Nilchiani, R.; Mostashari, A. Measuring the resilience of the global internet infrastructure system. *2009 3rd Annual IEEE Systems Conference*; IEEE. 2009.
- Henry, D.; Emmanuel Ramirez-Marquez, J. Generic metrics and quantitative approaches for system resilience as a function of time. *Reliab. Eng. Syst. Saf.* **2012**, *99*, 114–122.
- Baroud, H.; Ramirez-Marquez, J. E.; Barker, K.; Rocco, C. M. Stochastic Measures of Network Resilience: Applications to Waterway Commodity Flows. *Risk Anal.* **2012**, *34*, 1–122.
- Cho, S.; Li, C.; Grossmann, I. E. Recent advances and challenges in optimization models for expansion planning of power systems and reliability optimization. *Comput. Chem. Eng.* **2022**, *165*, 107924.
- Palma-behnke, R.; Abarca-del-rio, R. *The Chilean Potential for Exporting Renewable Energy*, 2021.
- Nahmmacher, P.; Schmid, E.; Hirth, L.; Knopf, B. Carpe diem: A novel approach to select representative days for long-term power system modeling. *Energy* **2016**, *112*, 430–442.
- Scott, I. J.; Carvalho, P. M.; Botterud, A.; Silva, C. A. Clustering representative days for power systems generation expansion planning: Capturing the effects of variable renewables and energy storage. *Appl. Energy* **2019**, *253*, 113603.
- Li, C.; Conejo, A. J.; Siirola, J. D.; Grossmann, I. E. On representative day selection for capacity expansion planning of power systems under extreme operating conditions. *Int. J. Electr. Power Energy Syst.* **2022**, *137*, 107697.
- Yeganefar, A.; Amin-Naseri, M. R.; Sheikh-El-Eslami, M. K. Improvement of representative days selection in power system planning by incorporating the extreme days of the net load to take account of the variability and intermittency of renewable resources. *Appl. Energy* **2020**, *272*, 115224.
- Molina, A.; Martínez, F.; Modelo de generación fotovoltaica, 2017.
- Wind Power in Power Systems; Ackermann, T., Ed.; John Wiley & Sons, Ltd, 2005.
- Afsharian, S.; Taylor, P. A. On the Potential Impact of Lake Erie Wind Farms on Water Temperatures and Mixed-Layer Depths: Some Preliminary 1-D Modeling Using COHERENS. *J. Geophys. Res.: Oceans* **2019**, *124*, 1736–1749.

- (35) Pamparana, G.; Kracht, W.; Haas, J.; Díaz-Ferrán, G.; Palma-Behnke, R.; Román, R. Integrating photovoltaic solar energy and a battery energy storage system to operate a semi-autogenous grinding mill. *J. Cleaner Prod.* **2017**, *165*, 273–280.
- (36) Corengia, M.; Torres, A. I. Effect of Tariff Policy and Battery Degradation on Optimal Energy Storage. *Processes* **2018**, *6*, 204.
- (37) Schmidt, O.; Gambhir, A.; Staffell, I.; Hawkes, A.; Nelson, J.; Few, S. Future cost and performance of water electrolysis: An expert elicitation study. *Int. J. Hydrogen Energy* **2017**, *42*, 30470–30492.
- (38) Proost, J. Critical assessment of the production scale required for fossil parity of green electrolytic hydrogen. *Int. J. Hydrogen Energy* **2020**, *45*, 17067–17075.
- (39) Martín, M. Optimal year-round production of DME from CO₂ and water using renewable energy. *J. CO₂ Util.* **2016**, *13*, 105–113.
- (40) El-Sharkh, M.; Tanrioven, M.; Rahman, A.; Alam, M. Cost related sensitivity analysis for optimal operation of a grid-parallel PEM fuel cell power plant. *J. Power Sources* **2006**, *161*, 1198–1207.
- (41) Saba, S. M.; Müller, M.; Robinius, M.; Stolten, D. The investment costs of electrolysis – A comparison of cost studies from the past 30 years. *Int. J. Hydrogen Energy* **2018**, *43*, 1209–1223.
- (42) You, S.; Hadley, S. W.; Shankar, M.; Liu, Y. Co-optimizing generation and transmission expansion with wind power in large-scale power grids—Implementation in the US Eastern Interconnection. *Electr. Power Syst. Res.* **2016**, *133*, 209–218.
- (43) Peyghami, S.; Wang, Z.; Blaabjerg, F. A Guideline for Reliability Prediction in Power Electronic Converters. *IEEE Trans. Power Electron.* **2020**, *35*, 10958–10968.
- (44) Kashefi Kaviani, A.; Riah, G.; Kouhsari, S. Optimal design of a reliable hydrogen-based stand-alone wind/PV generating system, considering component outages. *Renewable Energy* **2009**, *34*, 2380–2390.
- (45) Guilbert, D.; Collura, S. M.; Scipioni, A. DC/DC converter topologies for electrolyzers: State-of-the-art and remaining key issues. *Int. J. Hydrogen Energy* **2017**, *42*, 23966–23985.
- (46) Ministerio de Energía—Gobierno de Chile. Explorador Solar. Online, 2023, <https://solar.minenergia.cl/inicio> (accessed Aug 29, 2023).
- (47) Ministerio de Energía—Gobierno de Chile. Explorador eólico. 2023, <https://eolico.minenergia.cl/inicio> (accessed Aug 29, 2023).
- (48) Lane, B.; Reed, J.; Shaffer, B.; Samuelsen, S. Forecasting renewable hydrogen production technology shares under cost uncertainty. *Int. J. Hydrogen Energy* **2021**, *46*, 27293–27306.
- (49) Servicio de Impuestos Internos (SII). *Revalúo de Sitios no Edificados, Propiedades Abandonadas O Pozos Lastreros*, 2021.
- (50) Bynum, M. L.; Hackebel, G. A.; Hart, W. E.; Laird, C. D.; Nicholson, B. L.; Siirola, J. D.; Watson, J.-P.; Woodruff, D. L. *Pyomo—optimization Modeling in Python*, 3rd ed.; Springer Science & Business Media, 2021; Vol. 67.
- (51) Hart, W. E.; Watson, J.-P.; Woodruff, D. L. Pyomo: modeling and solving mathematical programs in Python. *Math. Program. Comput.* **2011**, *3*, 219–260.
- (52) Gurobi Optimization, L. L. C. *Gurobi Optimizer Reference Manual*. 2023.
- (53) Balas, E.; Jeroslow, R. Canonical Cuts on the Unit Hypercube. *SIAM J. Appl. Math.* **1972**, *23*, 61–69.
- (54) Ministerio de Energía—Gobierno de Chile. *Estrategia Nacional de Hidrógeno Verde*, 2020.